IOSR Journal of Computer Engineering (IOSR-JCE)
e-ISSN: 2278-0661, p-ISSN: 2278-8727, Volume 28, Issue 5, Ser. III (Sep. – Oct. 2026), PP 17-23
www.iosrjournals.org

Hemodynamic analysis of blood flow in an artery with atherosclerotic stenosis using the finite element method

Israel Isaac Gutiérrez Villegas[1-2], Julio Lara García[3], Belén de Jesús Gutiérrez Armenta[4], Esiquio Martín Gutiérrez Armenta[5], Marco Antonio Gutiérrez Villegas[6].

[1] División de Ingeniería en Sistemas Computacionales / Tese-TecNM, Av. Tecnológico S/N, Valle de Anáhuac, 55210 Ecatepec de Morelos, Edo. México, México.
[2]División Departamento de Ingeniería y Ciencias Sociales /ESFM. Instituto Politécnico Nacional (IPN). Av. Luis Enrique Erro S/N, Unidad Profesional Adolfo López Mateos, Zacatenco, Alcaldía Gustavo A. Madero, C.P. 07738, Ciudad de México.
[3]Ingeniería en Tecnologías de Manufactura e Ingeniería en Software. Prolongación 5 de Mayo #10, Colonia Felipe Villanueva, Centro Tecámac, CP 55740, Estado de México. México.
[4]QFI., Escuela Nacional de Ciencias Biológicas, IPN, Unidad Profesional Lázaro Cárdenas, Prolongación de Carpio y Plan de Ayala s/n, Col. Santo Tomás C.P. 11340 Alcaldía Miguel Hidalgo CDMX. México.
[5,6]Departamento de Sistemas, área de sistemas computacionales, Universidad Autónoma Metropolitana, Unidad Azcapotzalco, Av. San Pablo No. 420 Col. Nueva el Rosario C.P. 02128 Alcaldía Azcapotzalco, CDMX. México

Abstract: *A two-dimensional model is presented to compare blood flow in a reference artery and an artery with eccentric stenosis. LDL dynamics serve as the conceptual background; the artery's asymmetric contour was digitized and used to construct the finite element domain. The Navier-Stokes equations for an incompressible fluid were applied; blood was modeled as a Newtonian fluid with a density of 1060 kg/m³ and a viscosity of 0.0035 Pa·s. Boundary conditions included a mean velocity of 0.12 m/s, a no-slip condition at the walls, and zero gauge pressure at the outlet. A triangular mesh was applied separately to the upper and lower walls, without imposing symmetry. With fine discretization, the maximum velocity was 0.279 m/s and the pressure drop was 830.8 Pa (6.231 mmHg). The results show localized acceleration and an increased pressure gradient at the site of the obstruction. This is a computational study and does not constitute a clinical diagnosis.*

Background*: Atherosclerosis alters vascular geometry and, consequently, the velocity, pressure, and shear stress fields. Computational fluid dynamics enables the analysis of these variables under controlled conditions and complements experimental or clinical interpretation.*

Materials and Methods*: The contour of the original asymmetric artery was digitized and scaled to a length of 5.197 mm and a reference diameter of 1.142 mm. The maximum reduction in luminal height was approximately 62.5%. A Galerkin formulation with a penalty method for incompressibility and triangular elements was applied.*

Results*: The eccentric stenosis displaced and accelerated the flow core. Sensitivity analysis showed that velocity—and especially the pressure recovered via the penalty method—still depends on mesh refinement; therefore, these values are reported as preliminary numerical estimates.*

Conclusion: *The finite element model reproduces the expected physical trends of acceleration and pressure loss associated with a reduction in cross-sectional area. Geometric severity should be interpreted in conjunction with pulsatile flow, non-Newtonian rheology, and arterial distensibility in future models.*

Key Word*: Intrathecal; Hemodynamics; arterial stenosis; atherosclerosis; finite element method; Navier-Stokes; computational fluid dynamics.*

Date of Submission: 15-09-2026 Date of Acceptance: 29-09-2026

I. Introduction

Blood is a biological suspension composed of plasma and formed elements. In medium- and large-caliber arteries, and at sufficiently high shear rates, its behavior can be approximated using a constant viscosity; however, in regions of recirculation or in small vessels, non-Newtonian models become increasingly relevant. This distinction is essential because the choice of constitutive model determines the prediction of velocity, pressure, and wall shear stress. Bernoulli's principle states that when fluid exits a stenosis and enters an area of larger diameter, its velocity decreases, resulting in an increase in blood pressure.

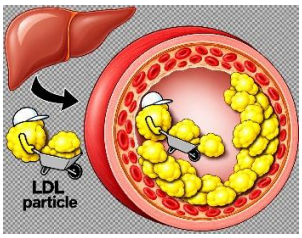

Figure 1. Accumulation of LDL cholesterol.

Hemodynamic parameters derived from simulations allow for the study of mechanisms linked to plaque progression, remodeling, and device performance. Their interpretation requires appropriate geometry, boundary conditions, and numerical verification8-13. The finite element method is particularly useful because it accommodates irregular domains, variational formulations, and local refinement. The objective of this work is to formulate and extend the analysis of an obstructed artery using a finite element method approach. A reference conduit is compared with one featuring mild stenosis; the governing equations, weak Galerkin formulation, discretization, boundary conditions, convergence analysis, and limitations are established. The contribution is methodological and educational; the numerical values correspond to an idealized model rather than a specific patient.

is a chronic inflammatory process of the arterial wall associated with lipoprotein retention, an immune response, and plaque formation. Elevated LDL cholesterol is a modifiable causal factor, but a stenosis should not be described simply as "solidified cholesterol"; the lesion comprises lipids, inflammatory cells, fibrous tissue, and frequently calcification. A drop in temperature alters hydraulic resistance, accelerates the pulse, and can trigger flow separation and blood recirculation downstream. is now commonly recognized as a coronary heart disease risk equivalent[1,2,3,4].This is mainly attributed to the high rates of dyslipidemia among diabetic patients which is believed to be one of the major factors accounting for the high percentage of deaths among diabetics due to cardiovascular disease (CVD)[5].Numerous epidemiological studies and randomized controlled trials have documented the association between elevated LDL-C levels with increased CVD risk in both diabetic and non-diabetic populations.[6,7]. Thus reducing LDL-C levels is the primary goal of therapy for diabetic dyslipidemia.[5,8].Statins are considered the first pharmacological line of treatment of dyslipidemia in diabetic patients[9]. Lowering of LDL-C levels is thought to be the main beneficial effect of statin treatment.In India currently no guidelines available for treating diabetic dyslipidemia and no previous study has documented the efficacy.The current study aims to build growing awareness of atherosclerosis specific care of diabetes patient by examining efficacy of two most commonly prescribed statins in India.

II. Material And Methods

This II.1 Domain geometry

A two-dimensional domain with a length of L = 5.197 mm and a reference diameter of D_0=1.142 = 1.142 mm was considered. The pixels for the upper and lower walls of the CFD (computational fluid dynamics) boundary were obtained independently. If $y_t(s)$ and $y_\beta(s)$ are digitized coordinates, h_0 is the reference luminal height, and c_0 is the centerline at the ends, the transformation to physical coordinates

$$Y_{SUP(X)} = \left[c_0 - y\_t\left(\frac{x}{L}\right)\right]\left(\frac{D_0}{h_0}\right) \ , \ y_{\inf(x)} = \left[c_0 - y\_b\left(\frac{x}{L}\right)\right]\left(\frac{D_0}{h_0}\right) \qquad (1)$$

This transformation preserves the plate's eccentricity: the upper part encroaches upon the clear opening to a greater extent than the lower part. No geometric symmetry was imposed. Figure 2 shows the original outline and the geometry digitized for the analysis.

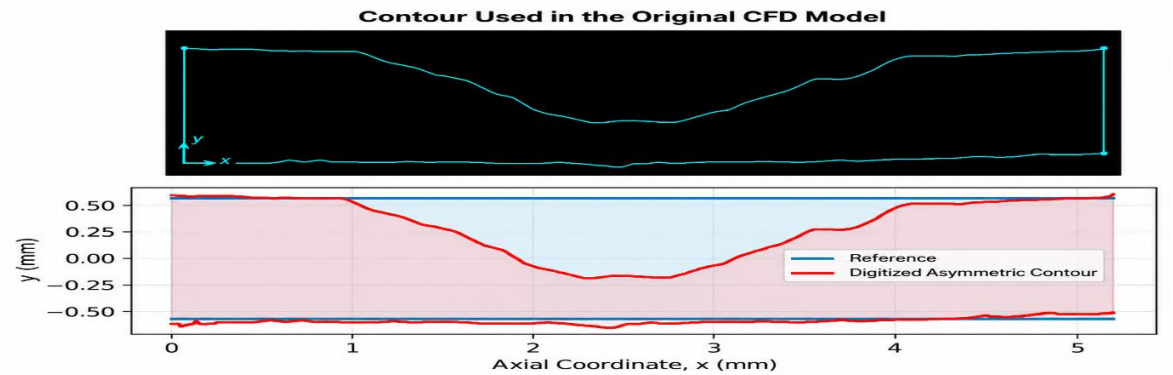

Figure 2. Asymmetric contour of the original CFD model and digitized reconstruction used as the domain for the FEM analysis. Prepared by the authors based on the figure provided by the author.

II.2. Governing equations and assumptions

The flow is considered steady, laminar, isothermal, and incompressible. The wall is modeled as rigid and the blood as Newtonian fluid. Under these assumptions, the conservation of mass and momentum is expressed as:

$$\nabla \cdot u = 0 \qquad (2)$$

$$\rho(u \cdot \nabla)u = -\nabla p + \mu\nabla^2 u \quad (3)$$

Where u is the velocity vector, p is the pressure, ρ is the density, and μ is the dynamic viscosity. The Reynolds number was estimated as $R_e = \frac{\rho \overline{U} D}{\mu}$; with $\overline{U} = 0.12\frac{m}{s}$, $D = 1.142\ mm$, $\rho = 1060\frac{kg}{m^3}$ and $\mu = 0.0035$ Pa·s, a value of $Re \approx 41.5$ is obtained, which is consistent with a laminar regime. Therefore, a k-ε model is not used.

II.3. Weak formulation and finite element discretization

By multiplying the equations by test functions v and q, integrating over the domain Ω, and applying integration by parts to the viscous term, the mixed formulation is obtained: to find (u, p) such that for all (v, q)

$$\int_\Omega \rho(u \cdot \nabla u)\, u \cdot v\, d\Omega + \int_\Omega 2\mu\, \varepsilon(u) : \varepsilon(v) d\Omega - \int_\Omega p\nabla \cdot v d\Omega = \int_{\Gamma_t} \bar{t} \cdot v\, d\Gamma \quad (4)$$

$$\int_\Omega q\nabla \cdot u\, d\Omega = 0 \quad (5)$$

With $\varepsilon(u) = (\nabla u + \nabla u^{\mathrm{T}})/2$. For the illustrative implementation, a penalty formulation was used $p \approx -\lambda\nabla \cdot u$ with λ sufficiently large relative to μ. The field was approximated using linear triangular shape functions N_i:

$$u\_h(x) = \Sigma_i N_i(x) u_i, \quad v\_h(x) = \Sigma_i N_i(x) v_i \qquad (6)$$

$$(K\_\mu + K\_\lambda)U = F \qquad (7)$$

The penalty method reduces the system to nodal velocity unknowns. For higher-fidelity studies, a stable inf-sup pairsuch as Taylor-Hood $P_2 - P_1$[1,2,17]or PSPG/SUPG[1-2-9]stabilization is recommended. Figure 3 shows the mesh in the constriction zone.

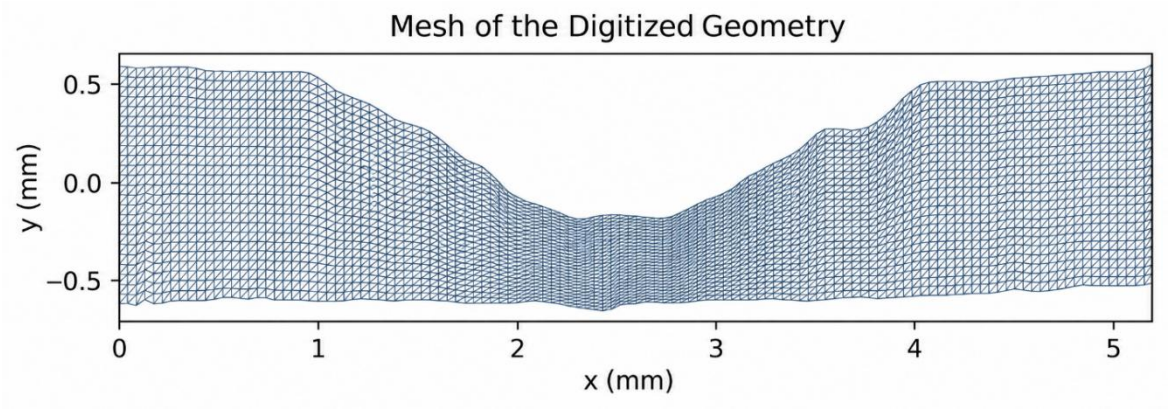

Figure 3. Triangular mesh of the stenotic domain, with an enlarged view of the throat

II.4. Properties, boundary conditions, and solution

Table no 1. Geometric parameters and properties used in the simulation.

Parameter	Symbol	Value	Unit
Arterial length	L	5.197	mm
Reference diameter	D_0	1.142	mm
Maximum reduction in luminal height	δ_h	62.5	%
Density	ρ	1060	kg/m³
Dynamic viscosity	μ	0.0035	Pa·s
Mean inlet velocity	$\overline{U}$	0.12	m/s
Reynolds number	Re	41.5	—

At the inlet, the parabolic profile $u_x(0,y) = 1.5U\left[1-\left(\frac{y}{R_0}\right)^2\right]$, u_y=0 were imposed. A no-slip condition $u = 0$ was applied at the walls, and a natural condition with a reference relative pressure $p = 0$ was set at the outlet. Exact integration was used for element gradients, along with a sparse solution method for the algebraic system.

$$u_x(0,y) = 1.5U\left[1-\left(\frac{y}{R_0}\right)^2\right],\ u_y=0. \quad (8)$$

II.5. Mesh sensitivity and output variables

Three discretization's with 2,560, 4,000, and 5,760 elements were compared. Maximum velocity and the pressure drop between the inlet and outlet were monitored. The variables examined were |u|, p, velocity along the geometric centerline, and pressure drop. Differences between meshes were used to quantify sensitivity and define the scope of the results, without assuming mesh independence when the 1% threshold was not met.

III. Result

III.1 Fields in the reference artery A smooth axial field was recovered in the unobstructed conduit. The profile imposed at the inlet evolved without local internal accelerations, and the pressure decreased gradually in the flow direction. The absence of abrupt changes in cross-section limits transverse gradients and prevents the formation of a localized central jet, as shown in Figure 4.

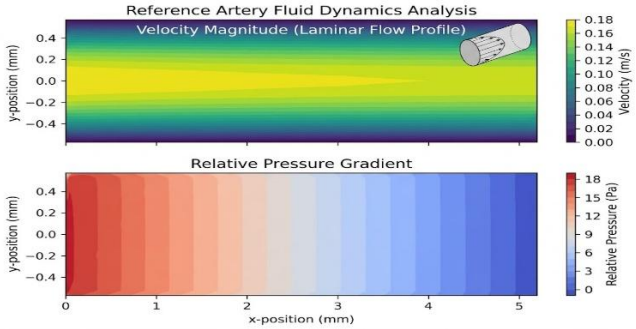

Figure 4. Velocity magnitude and relative pressure calculated using FEM in the reference artery.

III.2. Fields in the stenotic artery

The reduction in the lumen shifted the flow core toward the wall opposite the plaque and caused localized acceleration. With the fine mesh, the maximum velocity was 0.379 m/s. Relative pressure dropped across the lesion, with an overall decrease of 830.8 Pa, equivalent to 6.31 mmHg. These values were obtained from the digitized asymmetric geometry rather than an idealized symmetric stenosis.

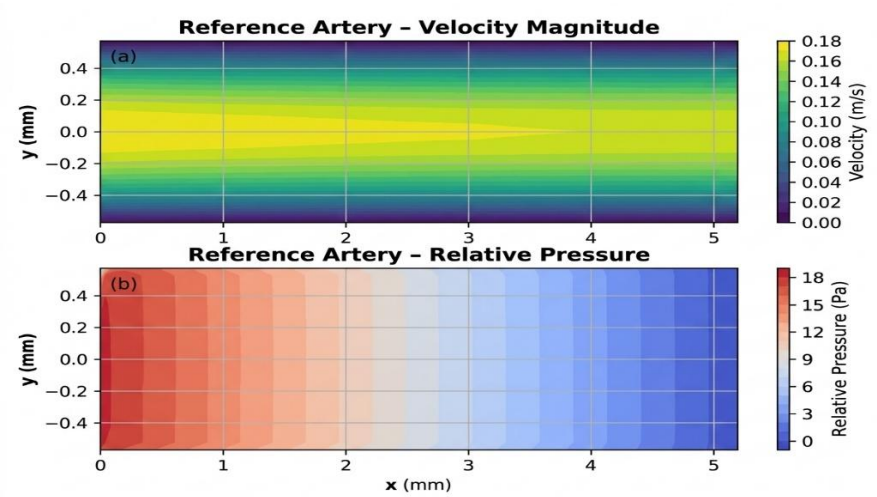

Figure 5. Velocity magnitude and relative pressure in the stenosed artery, obtained via FEM.

III.3.3 Comparison along the centerline

The axial velocity comparison aligns with the minimum cross-section. Downstream, the velocity decreases as the duct regains its diameter. The pressure gradient is most intense in the converging region and at the throat, reflecting the energy cost associated with the constriction Figure 6.

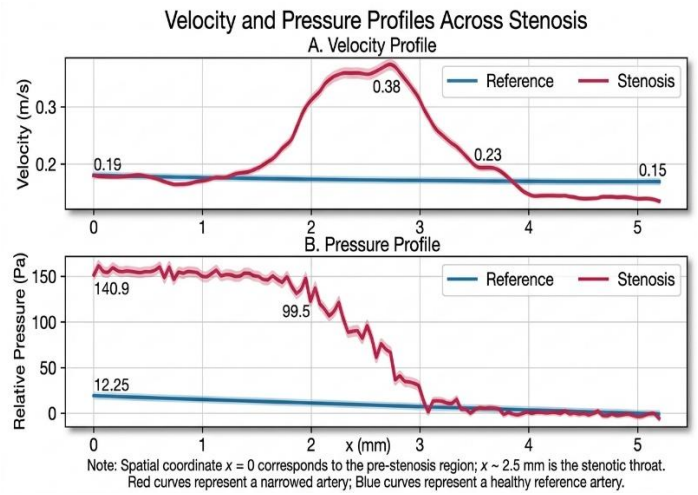

Figure 6. Velocity and relative pressure along the centerline for the two domains.

III.4. Mesh independence

Table no 2. Sensitivity to mesh refinement for the stenotic case, with pressure in Pa and mmHg.

	u_{max} (m/s)	Δp (Pa)	Δp (mmHg)	Elementos
2560	0.327	651.3	4.885	—
4000	0.361	665.9	4.994	10.53 %
5760	0.379	830.8	6.231	5.01 %

Between the two finest discretization's, the maximum velocity variation was 5.01% and the pressure drop variation was 24.77%. Table no 2 presents the pressure in both Pa and mmHg; the conversion 1 mmHg = 133.322 Pa was used. These differences indicate sensitivity regarding pressure recovery via the penalty method; therefore, the value obtained with the fine mesh is interpreted as an estimate rather than a mesh-independent solution. Figure 7 shows the observed trend.

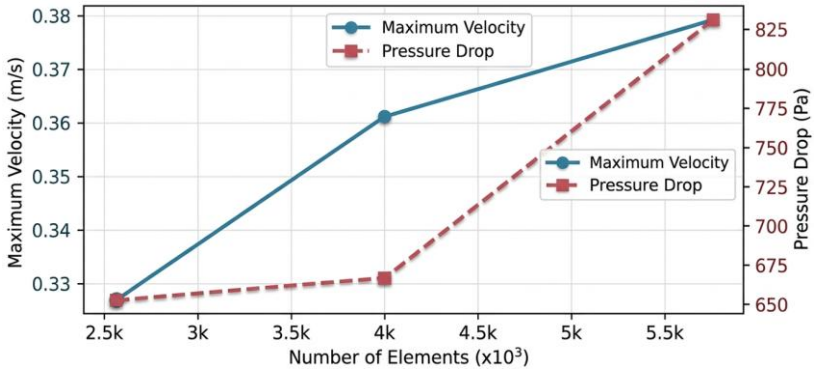

Figure 7. Sensitivity of maximum velocity and pressure drop to mesh refinement.

IV. Discussion

The acceleration at the throat and the increased pressure drop are consistent with mass conservation and computational studies of stenosed arteries10-16. However, the magnitude depends on the severity, shape, and length of the lesion, as well as the imposed flow rate. A quantitative comparison with a patient would require geometry segmented from medical imaging and specific inlet and outlet conditions.

The Newtonian assumption is reasonable as a first approximation for arteries of several millimeters in diameter and moderate-to-high shear rates. Carreau-Yasuda, Casson, or power-law models allow for the representation of shear-thinning behavior3-4-14. Furthermore, actual flow is pulsatile; the steady-state condition represents only an average state and does not provide temporal indices such as TAWSS or OSI.

The rigid-wall assumption precludes fluid-structure interaction. Vessel distensibility alters the pressure wave, stress distribution, and the phase relationship between pressure and flow12-15. A subsequent model should incorporate elastic or hyperelastic walls, time-dependent pressure, and inlet/outlet extensions sufficient to minimize boundary sensitivity.

While the use of a penalty formulation facilitates pedagogical implementation, it does not replace a stable mixed discretization for clinical simulations; significant improvements would include employing Taylor-Hood P_2–P_1 elements, demonstrating mass balance, conducting a sensitivity analysis regarding λ, and performing validation against Poiseuille flow or experimental data.

The results do not support the claim that an obstruction can be detected solely by measuring pressure or velocity over "short distances." Clinical utility depends on the imaging modality, resolution, vascular location, and integration with medical criteria. Simulation should be viewed as a complementary tool rather than a standalone diagnostic method.

V. Conclusion

A blood flow formulation was developed using the finite element method, incorporating the asymmetric contour of the obstructed artery. Independent digitization of both walls avoided imposing a symmetry that does not exist in the plaque. Under the conditions analyzed, the model yielded a maximum velocity of 0.279 m/s and a pressure drop of 830.8 Pa (6.231 mmHg). Comparison with a reference artery made it possible to identify the displacement of the velocity core and the hydraulic effect of the eccentric constriction.

References

[1] Formaggia, L., Quarteroni, A. y Veneziani, A. (Eds.). Cardiovascular Mathematics: Modeling and Simulation of the Circulatory System. Springer, 2009. https://doi.org/10.1007/978-88-470-1152-6

[2] Quarteroni, A., Manzoni, A. y Vergara, C. The cardiovascular system: Mathematical modelling, numerical algorithms and clinical applications. Acta Numerica, 26, 365–590, 2017. https://doi.org/10.1017/S0962492917000046

[3] Gijsen, F. J. H., van de Vosse, F. N. y Janssen, J. D. The influence of the non-Newtonian properties of blood on the flow in large arteries. Journal of Biomechanics, 32(6), 601–608, 1999. https://doi.org/10.1016/S0021-9290(99)00015-9

[4] Stamou, A. C. et al. A comparison of Newtonian and non-Newtonian models for blood flow simulations. Fluids, 8(10), 282, 2023. https://doi.org/10.3390/fluids8100282

[5] Libby, P. The changing landscape of atherosclerosis. Nature, 592, 524–533, 2021. https://doi.org/10.1038/s41586-021-03392-8

[6] Borén, J. et al. Low-density lipoproteins cause atherosclerotic cardiovascular disease: pathophysiological, genetic, and therapeutic insights. European Heart Journal, 41(24), 2313–2330, 2020. https://doi.org/10.1093/eurheartj/ehz962

[7] Visseren, F. L. J. et al. 2021 ESC Guidelines on cardiovascular disease prevention in clinical practice. European Heart Journal, 42(34), 3227–3337, 2021. https://doi.org/10.1093/eurheartj/ehab484

[8] Steinman, D. A. Image-based computational fluid dynamics modeling in realistic arterial geometries. Annals of Biomedical Engineering, 30, 483–497, 2002. https://doi.org/10.1114/1.1467679

[9] Taylor, C. A. y Figueroa, C. A. Patient-specific modeling of cardiovascular mechanics. Annual Review of Biomedical Engineering, 11, 109–134, 2009. https://doi.org/10.1146/annurev.bioeng.10.061807.160521

[10] Lopes, D. et al. Analysis of finite element and finite volume methods for fluid-structure interaction simulation of blood flow in a real stenosed artery. International Journal of Mechanical Sciences, 2021. https://doi.org/10.1016/j.ijmecsci.2021.106650

[11] Wang, L. et al. Fast prediction of blood flow in stenosed arteries using physics-informed and data-driven methods. Frontiers in Physiology, 13, 953702, 2022. https://doi.org/10.3389/fphys.2022.953702

[12] Shahzad, H. et al. Study of non-Newtonian biomagnetic blood flow in a stenosed bifurcated artery having elastic walls. Scientific Reports, 11, 23835, 2021. https://doi.org/10.1038/s41598-021-03426-1

[13] Nadeem, S. et al. Numerical computations of blood flow through stenosed arteries. Alexandria Engineering Journal, 2023. https://doi.org/10.1016/j.aej.2023.02.005

[14] Nejad, A. A. et al. Pulsatile flow of non-Newtonian blood fluid inside stenosed arteries: investigating the effects of viscoelastic and elastic walls, arteriosclerosis, and polycythemia diseases. Computer Methods and Programs in Biomedicine, 154, 109–122, 2018. https://doi.org/10.1016/j.cmpb.2017.11.016

[15] Pabi, S. et al. Hemodynamics and thermal characteristics of a deformable stenosed carotid artery with heat generation: effect of heart rate, stenotic severity, and wall elasticity. International Communications in Heat and Mass Transfer, 2024. https://doi.org/10.1016/j.icheatmasstransfer.2024.108236

[16] Praharaj, P. et al. Numerical analysis of hemodynamic parameters in stenosed arteries under pulsatile flow conditions. Medicine in Novel Technology and Devices, 19, 100265, 2023. https://doi.org/10.1016/j.medntd.2023.100265

[17] Donea, J. y Huerta, A. Finite Element Methods for Flow Problems. Wiley, 2003.

[18] Hughes, T. J. R. The Finite Element Method: Linear Static and Dynamic Finite Element Analysis. Dover Publications, 2000.